Revised Manuscript sent to C.J.Ch.E

Energy, Mines and Resources Canada | Énergie, Mines et Ressources Canada

CANMET

Canada Centre for Mineral and Energy Technology | Centre canadien de la technologie des minéraux et de l'énergie

PREPARATION OF HIGH POROSITY CATALYSTS

M. Ternan, R.H. Packwood, R.M. Buchanan and B.I. Parsons

November 1980

ENERGY RESEARCH PROGRAM

ENERGY RESEARCH LABORATORIES

REPORT ERP/ERL 80-82(J)

ERP/ERL 80-82 (J)

PREPARATION OF HIGH POROSITY CATALYSTS[1]

by

M. Ternan, R.H. Packwood, R.M. Buchanan and B.I. Parsons
Energy Research Laboratories
Department of Energy, Mines and Resources
Ottawa, Ontario K1A 0G1

ABSTRACT

Porous alumina catalyst supports have been prepared with pore volumes exceeding 1.0 mL/g, with most pores having diameters of the order of 3 micrometers and with surface areas exceeding 150 m^2/g. They were obtained from dilute alumina gels having large concentrations of acid and very large concentrations of fluid. Attempts were made to dry the gel without collapsing the pore structure between the alumina particles. The catalysts were characterized by gravimetrical BET surface area, mercury porosimetry, X-ray diffraction and scanning electron microscopy. Catalyst supports having these geometric properties should eliminate mass transfer restrictions during hydrocracking of petroleum residua, heavy oils and bitumen derived from oil sand deposits.

---

[1]Presented at the 7th Canadian Symposium on Catalysis, Edmonton, Alberta, Oct. 19-22, 1980.

For some time research in our laboratories has been directed toward hydrocracking bitumen derived from oil sand deposits, heavy oil and residuum. Conventional catalysts used for hydrotreating and for hydrocracking residual oils often have pore diameters around 7 nm. It is widely recognized that pores larger than these are desirable for hydrocracking residual oils.

Considerable work (1) has been performed in order to better define the optimum pore size. There are at least two reasons for the desirability for larger pores. First, it is generally recognized that the rate of reaction is limited by the rate at which large molecules diffuse within the catalyst structure. Increasing the pore size tends to decrease or eliminate diffusional restrictions. Newson (2) has described this phenomenon theoretically. Secondly, it is known that metals are preferentially deposited near the outside of catalyst pellets or extrudates when catalysts having small pores are employed. If catalysts with sufficiently large pores are used, it should be possible for these poisons to be dispersed more uniformally throughout the catalyst. This should decrease or eliminate pore mouth plugging and therefore prolong the useful life of the catalyst.

Previous work in this laboratory involved the study of large pore catalysts which were made by sintering (3). Sintering also causes a loss in surface area. Unfortunately in that study, the catalysts with the largest pore sizes which were of primary interest also had extremely low surface areas.

The present work was directed toward the development of large pore catalysts which also had large surface areas. The general approach involved two steps. First, attempts were made to prepare colloidal alumina gels having large interstitial volumes which were filled with water. Second, attempts were made to remove the water without causing the alumina structures to collapse.

There is a considerable amount of literature describing gels qualitatively (4). Gels (5) are formed by particles which unite to make short chains or threads. These become tangled and form a semi-solid. The major portion of the water in gels is held by capillary forces between the solid threads.

The approach in this work was to increase the amount of capillary held water thereby attempting to increase the dimensions of the capillaries. It is known (6) that the addition of acid will sometimes help to stabilize gels. As a result both variables, the amount of water and the amount of acid were investigated.

The procedure used to remove the water from the capillaries within the gel is very important. Kistler (7) noted that during removal of liquid from a capillary within a gel, the surface tension at the gas-liquid interface acts on the solid and causes the solid structure in the gel to collapse. This phenomenon can be suppressed by using a solvent other than water, which has a lower gas-liquid surface tension. Unfortunately the cost of such solvents with the requirement for solvent recovery introduces undesirable complexities into catalyst manufacturing. Another approach has been to remove the solvent at conditions above its critical point. This totally eliminates the gas-liquid interface. Teichner and coworkers (8) have used this method extensively. Organic solvents must also be used in this case since water at high temperature dissolves many oxides. Subsequently the oxides come out of solution in the form of crystals. Crystalline solids have low surface areas and are undesirable for catalytic purposes.

Shaw and Parsons (9) developed a procedure consisting of precipitation, washing-filtering and low temperature drying which resulted in highly porous catalysts. In this work low temperature drying was employed. However, the inconvenience of precipitation, washing and filtering was avoided by using a readily available type of alpha alumina monohydrate (boehmite).

EXPERIMENTAL

Two series of gels having the compositions shown in Tables 1 and 2 were prepared. The boehmite was Catapal SB alumina monohydrate purchased from the Continental Oil Company. Reagent grade 70 wt % nitric acid purchased from Allied Chemical was used. In each case distilled water was added to the weighed amount of boehmite first, followed by the addition of acid. After mixing, the material was allowed to stand for twenty-four hours. It was then dried at 333 K until no further weight loss occurred. Subsequently it was calcined at 773 K for six hours.

Several techniques were used to characterize the resulting materials. BET surface areas were measured by nitrogen adsorption using a gravimetric technique. A Micromeritics Model 915-1 mercury porosimeter was used to measure catalyst pore diameter. The contact angle between the mercury and the solid was assumed to be 130 degrees for both penetration and retraction. The X-ray diffraction measurements were made using a North American Phillip's X-ray diffractometer Model No. 42237/1. A proportional counter detector, a cobalt tube and an iron filter were used. Photographs of the material were taken with a Cambridge S2A Scanning Electron Microscope. The micrographs shown were obtained in secondary electron mode at 3.2 fJ. The sample surfaces were rendered conducting by sequentially evapourating coatings of carbon (approx. 20 nm) and gold (approx. 10 nm).

RESULTS

Gels developed gradually after the components were mixed during the first step in the preparation. The types of gel obtained are listed in Tables 1 and 2. Table 1 shows that the gels became less firm (less viscous) as the proportion of water in the mixture increased. Table 2 shows that increasing the proportion of nitric acid in the mixture had a complex effect on the gel condition.

A uniform gel would indicate that all the solution was associated with the solid. In contrast, a two phase mixture indicated that some of the solution was separate from the solid.

The porosities of all the resulting solids were measured by mercury porosimetry. Two examples are shown in Figs. 1 and 2. Figure 1 shows that most of the porosity in Catalyst D is in small pores. This range of pore size is typical of those found in conventional hydrotreating catalysts. Figure 2 shows that most of the porosity in sample J is in large pores. This range of pore size is typical of that in the high porosity catalyst examined in this study. For present purposes small pores are defined as pores having diameters of 3.5 to 10 nm. The pore diameters were those obtained from mercury penetration.

The geometrical properties of the two series of catalysts are displayed in Figures 3 and 4. Figure 3 shows the series of catalysts prepared

with various amounts of water. The surface area, small pore volume and large pore volume of the calcined catalysts increased as the amount of water in the original preparation mixture increased. Some of the small pore volume developed during the drying step, but most developed during calcining. The large pore volume was essentially the same after drying and after calcining. A large increase in the large pore volume occurred in the catalyst made with the greatest quantity of water.

Figure 4 shows the series of catalysts prepared with various amounts of nitric acid. Although somewhat scattered the data show an increase in surface area, a decrease in small pore volume, and an increase in large pore volume with increasing nitric acid. The magnitude of the large pore volume in Figure 4 is approximately four times greater than that shown in Figure 3.

X-ray diffraction results for the dried samples are shown in Figure 5. The materials obtained after drying two of the gels made with different amounts of water (which eventually became samples A and D after calcining) produced curve K. Curve K is very obviously the diffraction pattern for alpha alumina monohydrate (boehmite). It is not surprising to learn that gels made from mixtures of boehmite and water are transformed into boehmite upon drying.

The X-ray diffraction pattern for the material obtained after drying the gel made with the largest amount of nitric acid (which eventually became sample J after calcining) produced curve M. Some of the peaks in this curve correspond to those in the alumina trihydrates (gibbsite and bayerite). The diffraction pattern for aluminum nitrate is also shown in Figure 5. This pattern certainly is not that of sample M. However, aluminum nitrate crystals containing different waters of hydration might produce different diffraction patterns. One could speculate that sample M was composed of a mixture of alumina trihydrates and aluminum nitrates with different waters of hydration.

In an attempt to understand the development of the crystal structure, sample M was subsequently dried further at 110°C and its X-ray diffraction pattern measured. The material was extremely amorphorus. The only peaks obtained were at low angles corresponding to lattice spacings of 0.83 nm and 1.04 nm. This may have been indicative of pore dimensions rather

than lattice spacings.

Some of the X-ray diffraction results for the calcined catalysts are shown in Figure 6. The most intense peak obtained from the gel made with the least amount of water (calcined catalyst D) is shown in the figure. Other less intense peaks were observed close to incidence angles of 43.3 and 37.4 degrees. These values suggest that catalyst D is gamma alumina. Catalyst E, the one prepared using the largest quantity of water, gave an X-ray diffraction spectrum which was essentially the same as the one for catalyst D. The intensity of the peak in Figure 6 for catalyst J (the one made using the largest quantity of acid) is much lower. Furthermore, no other peaks could be identified. This suggests that catalyst J may be a very amorphous form of gamma alumina. Alternatively, it could be eta alumina. Both gamma and eta aluminas have their most intense peaks at the same incidence angle, but the one for eta alumina is less intense (10).

Low magnification scanning electron micrographs of some of the dried samples are shown in Figure 7. The top (sample K) and middle (sample L) micrographs show that the size of the particles formed after drying increases as the amount of water in the gel increases. Presumably small pores would form within the particles and large pores will form in the spaces between the particles. If the particle dimensions would persist after calcining, then the larger the particles the greater would be the dimensions of the large pores between the particles. The bottom micrograph (sample M) shows that crystalline material was obtained after drying the gel formed with the greatest amount of acid. Sample M was not a stable material. It would pick up moisture when left exposed to the atmosphere. When in the electron microscope, the electron beam tended to cause the sample to dehydrate.

Low magnification scanning electron micrographs of some of the calcined catalysts are shown in Figure 8. The top micrograph (sample D) indicates that the surface is rather flat at low magnification, although our investigation and other literature studies (11,12) indicate that gamma alumina is actually composed of particles which are too small to be seen at the magnification of Figure 8. Our high magnification micrographs were of poor quality due to sample charging. The black line running across the micro-

graph in Figure 8 is a crack in the alumina. The middle micrograph (sample E) shows that this sample is composed of spherical particles. The spaces between these particles are undoubtedly the large pores in Figure 3. After comparing the top and middle micrographs it is apparent that increasing the amount of water in the gel causes a large increase in the alumina particle size in the final calcined product. The bottom micrograph (sample J) shows a structure consisting of hollow tubes or shells. The alumina being the material which forms the walls. These tube or shell interiors are undoubtedly the large pores shown in Figure 4.

DISCUSSION

An explanation of the gel-formation processes begins with the structure of alpha monohydrate (boehmite), from which the gels were prepared. Wilson (13) ascribed the idealized structure in Figure 9 to boehmite. The dotted lines in Figure 9b illustrate hydrogen bonding between the layers. When water is added to boehmite to form a gel, the water molecules are located between the layers of boehmite, as shown in Figure 10. Hydrogen bonding occurs among water molecules and the surfaces of the boehmite. As the amount of water in the gel increases the thickness of the water layer in Figure 10 will increase. Eventually the gel will accomodate no more water between the boehmite layers. A gel phase and a solvent phase will be formed. The free energy of the system will be minimized by minimizing the interfacial area between the phases. Spheres of gel should be formed in the water solvent. Iler (6) has noted that gels made from dilute reagents produce larger primary particles. This picture is consistent with the micrographs in Figure 7 which showed that increasing the amount of water in the gel produced larger boehmite particles after drying.

Increasing the acid content increases the stability of the gel (6) as observed in Table 2. The presence of acid might be expected to improve hydrogen bonding in the water layers between the boehmite layers shown in Figure 10. However, at some point the boehmite undergoes a phase change. Figures 5M and 7 (bottom) clearly show that drying the acid treated gel produces a material which is substantially different than boehmite. The X-ray diffraction pattern for the dried material has some of the major peaks found

in $Al_2O_3.9H_2O$ and in beta alumina trihydrate (bayerite). However, it also contains many other peaks. Perhaps the other peaks are produced by crystals having different numbers of hydrated water molecules. It seems reasonable that acid would transform boehmite into bayerite, since Gitzen (14) has reported that the reverse transformation is accomplished by base. Also Calvet and Thibon (15) have reported that alpha alumina monohydrate (boehmite) can be rehydrated to beta alumina trihydrate (bayerite). Yoldas (16) and Schmit and Milligan (17) have shown that boehmite can be transformed into bayerite at different conditons.

In this work removal of water from the gel was accomplished by low temperature drying. This technique avoids the collapse of the pore structure which Kistler (7) attributed to surface tension forces between capillary held liquid and the solid. Low temperature drying is different from high temperature drying in at least two ways. Theory (18) indicates that at temperatures above the boiling point of the solvent, the rate of drying is controlled by the rate at which heat is transferred to the solid. Water is probably evapourated near its original location in the solid. The gas-liquid interfaces created throughout the solid probably cause the capillaries within the gel to collapse. At temperatures below the boiling point of the solvent, water diffuses from the interior of the solid and evapourates at the solid exterior. In this case after water has been removed from the capillaries, a multilayer (a few molecules thick) of water will be left on the surface of the solid. The multilayers may prevent the transfer of surface tension forces from the capilliary gas-liquid interface to the solid, thereby suppressing the collapse of the capillaries.

The second difference between low and high temperature drying involves mechanical forces. Usually the solids are dried at a total pressure near one atmosphere in a gaseous environment of air and water vapour. The numerical value of the water vapour pressure increases as a function of temperature. If the solid temperature exceeds the boiling point of the water solvent (100°C) two possibilities exist. When all the water is in the vapour phase, superheated steam will be present. If the capillaries contain

water in the liquid phase, it will be at the same temperature as the solid (above the boiling point) and the vapour pressure will exceed one atmosphere. The pressure in excess of one atmosphere will produce a force on the solid and tend to compress the parts of the solid which are filled with vapour. In contrast, during low temperature drying, the solid temperature cannot exceed the boiling point of the water solvent. Therefore, the pressure in the liquid phase will always be less than one atmosphere, and no forces causing pore collapse will result.

The removal of capillary held water from the gel will be influenced by the relative pressure of the water vapour and the dimensions of the capillary. The Kelvin equation shows that water should be removed from large pores before it is removed from small pores. The data in Figure 3 after drying and after calcining can be compared in this context. Low temperature drying removed all of the water from the large pores, since the large pore volumes were the same before and after calcining. However, low temperature did not remove all the water from the small pores, since the small pore volume increased considerably after calcining. This shows clearly that the function of low temperature drying is to remove water from the large pores.

The calcining step removes the water from the small pores, as shown in Figure 3, thereby developing the dehydration pores described by Johnson and Mooi (12). The transformation of boehmite to gamma alumina (10,14,19) also occurs during calcining. This transformation occurred in the catalysts which did not contain large amounts of acid, as can be seen by comparing Figures 5 and 6.

The phase transformations during calcining are more difficult to identify in the catalysts containing large amounts of acid. The X-ray diffraction pattern indicates the presence of either amorphorus gamma alumina or eta alumina. Figure 4 shows that the calcined form of the acid catalysts does not contain any small pores. It is, therefore, a different material than the gamma alumina which has a considerable quantity of small pores (12,13) as shown in Figure 3. Eta alumina is therefore a realistic possibility. Stumpf et al (10) have shown that eta alumina is formed from beta alumina trihydrate (bayerite). Perhaps bayerite is formed from the dried acid gel during the initial heating stage during calcining. The curvature

of the calcined product (tubes or shells) shown in Figure 8 is consistent with the finding of Schmit and Milligan (17) that rolled sheets resembling Halloysite were formed from bayerite. Also, beta alumina trihydrate (bayerite) is formed by rapid precipitation from sodium aluminate (10). Shaw and Parsons (9) used a similar technique to produce a highly porous catalyst.

The calcined catalysts made from acid gels do not contain small pores. In spite of this Figure 4 shows that their surface areas remain large. This suggests that the walls of the tubes or shells in Figure 8 are composed of very small particles. It is possible that the pores, formed from spaces between these particles, are too small to be measured by mercury porosimetry.

CONCLUSIONS

Highly porous catalyst supports have been prepared from dilute alumina gels. Attempts were made to remove the fluid, separating the alumina particles in the gel, without collapsing the pore structure between the particles. Large acid concentrations and very large fluid concentrations favored the preparation of highly porous solids. These solids were found to have both large pore diameter and large surface areas. On the basis of previous work (3) it is apparent that these pore diameters considerably exceed those at which reaction rates of large hydrocarbon molecules and micelles are limited by diffusional restrictions. Solids having this pore structure should find application as catalyst supports for hydrocracking petroleum residua, heavy oils and bitumen derived from oil sand deposits.

REFERENCES

1. Richardson, R.L. and Starling, K.A. "Hydrocracking and Hydrotreating"; ACS Symposium Series, No. 20 (eds. J.W. Ward and S.A. Qader); Am. Chem. Soc., Washington, D.C., p. 136; 1975.

2. Newson, E. Preprints; Am. Chem. Soc. Div. Petrol. Chem. 17(2), 49 (1972).

3. Hardin, A.H., Packwood, R.H. and Ternan, M. Preprints; Am. Chem. Soc. Div. Petrol. Chem. 23(4), 1450 (1978).

4. Hermans, P.H. in Colloid Science (ed. H.R. Krupt); v. 2; Elsevier, Amsterdam; p. 483; 1949.

5. Glasstone S. and Lewis D. "Elements of Physical Chemistry"; 2nd ed; Van Nostrand, Princeton; p. 586; 1960.

6. Iler, R.K. "The Colloid Chemistry of Silica and Silicates"; Cornell University Press; Ithaca; p. 44-54; 1955.

7. Kistler, S., J. Phys. Chem. 36,52 (1932).

8. Teichner, S.J., Nicolaon, G.A., Vicarini, M.A. and Gardes, G.E.E. Adv. Colloid Interf. Sci. 5,246 (1976).

9. Shaw, G.T. and Parsons, B.I. "Low Density Catalysts and Catalyst Supports Part 1: The Preparation of Highly Porous Alumina"; Mines Branch; Research Report R 199; Department of Energy, Mines and Resources, Ottawa; 1968.

10. Stumpf, H.C., Russel, A.S., Newsome, J.W. and Tucker, C.M., Ind. Eng. Chem. 42,1398 (1950).

11. Turkevitch, J. and Hillier, J., Anal. Chem. 21,475 (1949).

12. Johnson, M.F.L. and Mooi, J., J. Catal. 10,342 (1968).

13. Wilson, S.J., Mineralogical Magazine 43,301 (1979).

14. Gitzen, W.H. "Alumina as a Ceramic Material"; Am. Ceram. Soc. Columbus, Ohio; p. 17; 1979.

15. Calvet, E. and Thibon, H., Bull. Soc. Chim. 1343 (1954).

16. Yoldas, B.E., J. Appl. Chem. Biotechnol. 23, 803 (1973).

17. Schmit, P.W. and Milligan, W.D., J. Electronmicros. 10,238 (1961).

18. Treybal, R.E., "Mass Transfer Operations"; 2nd ed; McGraw-Hill; New York; p. 613; 1968.

19. Lippens, B.C. and Steggerda, J.J., "Physical and Chemical Aspects of Adsorbents and Catalysts"; (ed. B.G. Linsen); Academic Press, New York; p. 189; 1970.

FIGURE CAPTIONS

Figure 1 Pore volume (mL/g) versus pore diameter (nm) or applied pressure of mercury (MPa) for sample D after calcining. Squares and circles are for penetration and retraction respectively.

Figure 2 Pore volume (mL/g) versus pore diameter (nm) or applied pressure of mercury (MPa) for sample J after calcining. Squares and circles are for penetration and retraction respectively.

Figure 3 Surface area (m^2/g), volume of 3.5-10 nm micropores (mL/g) and volume of 1-50 μm macropores (mL/g) versus amount of water (wt %) add to the gel mixture. Square data points were obtained after drying. Circular data points were obtained after calcining.

Figure 4 Surface area (m^2/g), volume of 3.5-10 nm micropores (mL/g) and volume of 1-50 μm macropores (mL/g) versus amount of water (wt %) in calcined gel mixture.

Figure 5 X-ray diffraction pattern, relative intensity versus incidence angle: 2θ for dried samples K (which became D after calcining) and M (which became J after calcining).

Figure 6 X-ray diffraction pattern, relative intensity versus incidence angle: 2θ for calcined samples D and J.

Figure 7 Scanning electron micrograph of dried samples: Top - Sample K (which became sample D after calcining) obtained for the gel having the smallest amount of water. Middle - Sample L (which became sample E after calcining) obtained from the gel having the largest amount of water. Bottom - Sample M (which became Sample J after calcining) obtained from the gel having the largest amount of nitric acid.

Figure 8 Scanning electron micrograph of calcined samples. Top - Sample D obtained from the gel having the smallest amount of water. Middle - Sample E obtained from the gel having the largest amount of water. Bottom - Sample J obtained from the gel having the largest amount of nitric acid.

Figure 9 The structure of boehmite. (a) A three dimensional representation of part of a boehmite layer. (b) A two dimensional representation of boehmite layers. The dotted lines represent hydrogen bonding between the layers. (c) Wilson's representation of boehmite.

Figure 10 Hydrogen bonding of water molecules between boehmite layers.

Table 1 - Porous catalysts prepared with various amounts of water

Catalyst Identification	Boehmite wt %	Water wt %	70% HNO_3 wt %	Gel Condition
A	9.4	85.2	5.4	very watery
B	15.6	79.1	5.3	watery
C	32.4	65.3	2.3	firm
D	49.7	49.6	0.7	firm

Table 2 - Porous catalysts prepared with various amounts of 70% HNO_3

Catalyst Identification	Boehmite wt %	Water wt %	70% HNO_3 wt %	Gel Condition
E	9.1	90.9	-	no gel formed
F	8.7	86.7	4.6	firm gel
G	8.1	80.5	11.4	watery gel
H	6.5	64.9	28.6	clear solution plus firm gel
J	6.6	-	93.4	crusty solid surface

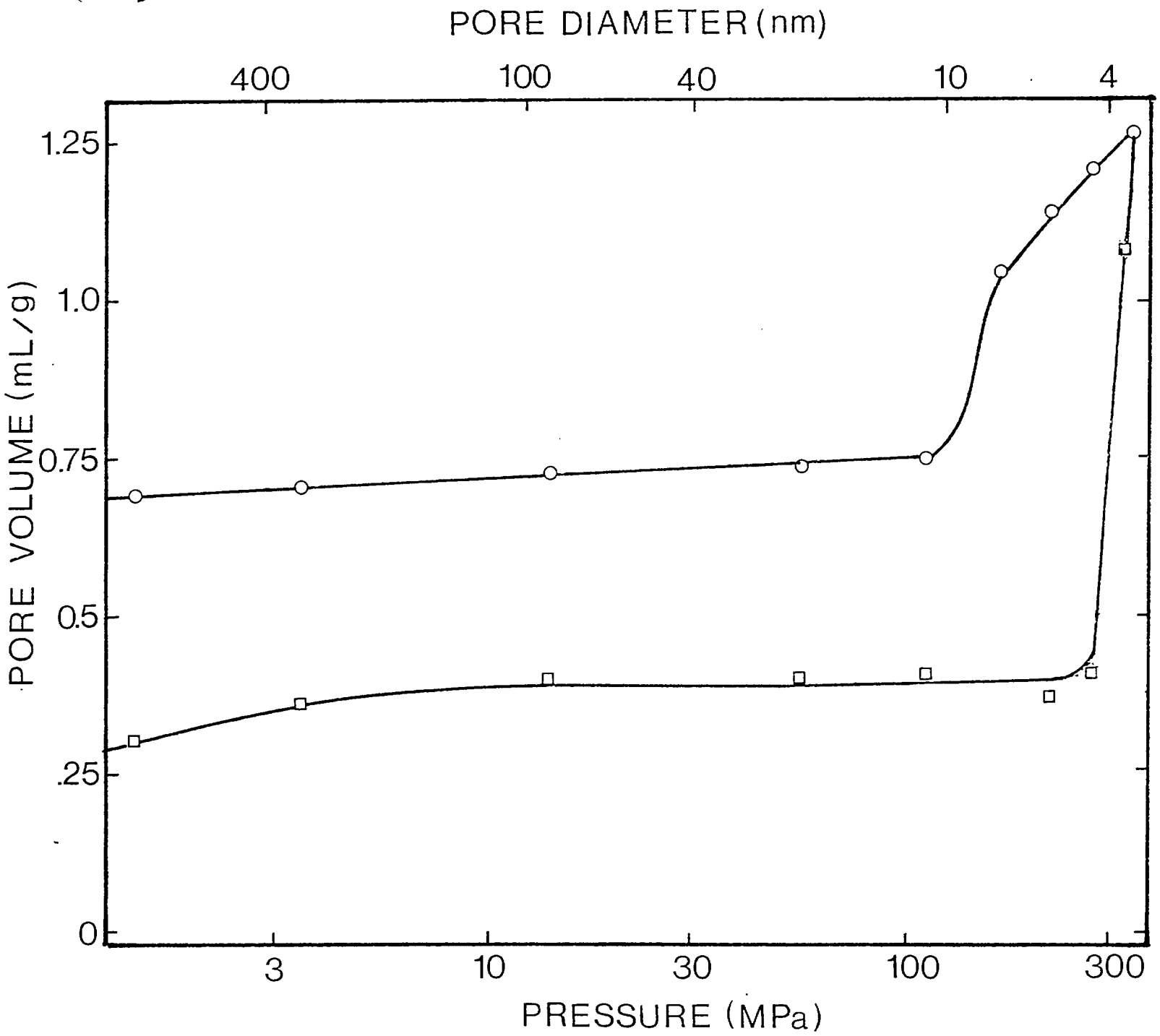
PORE DIAMETER (nm)
400
100
40
10
4
1.25
1.0
0.75
0.5
.25
0
PORE VOLUME (mL/g)
3
10
30
100
300
PRESSURE (MPa)

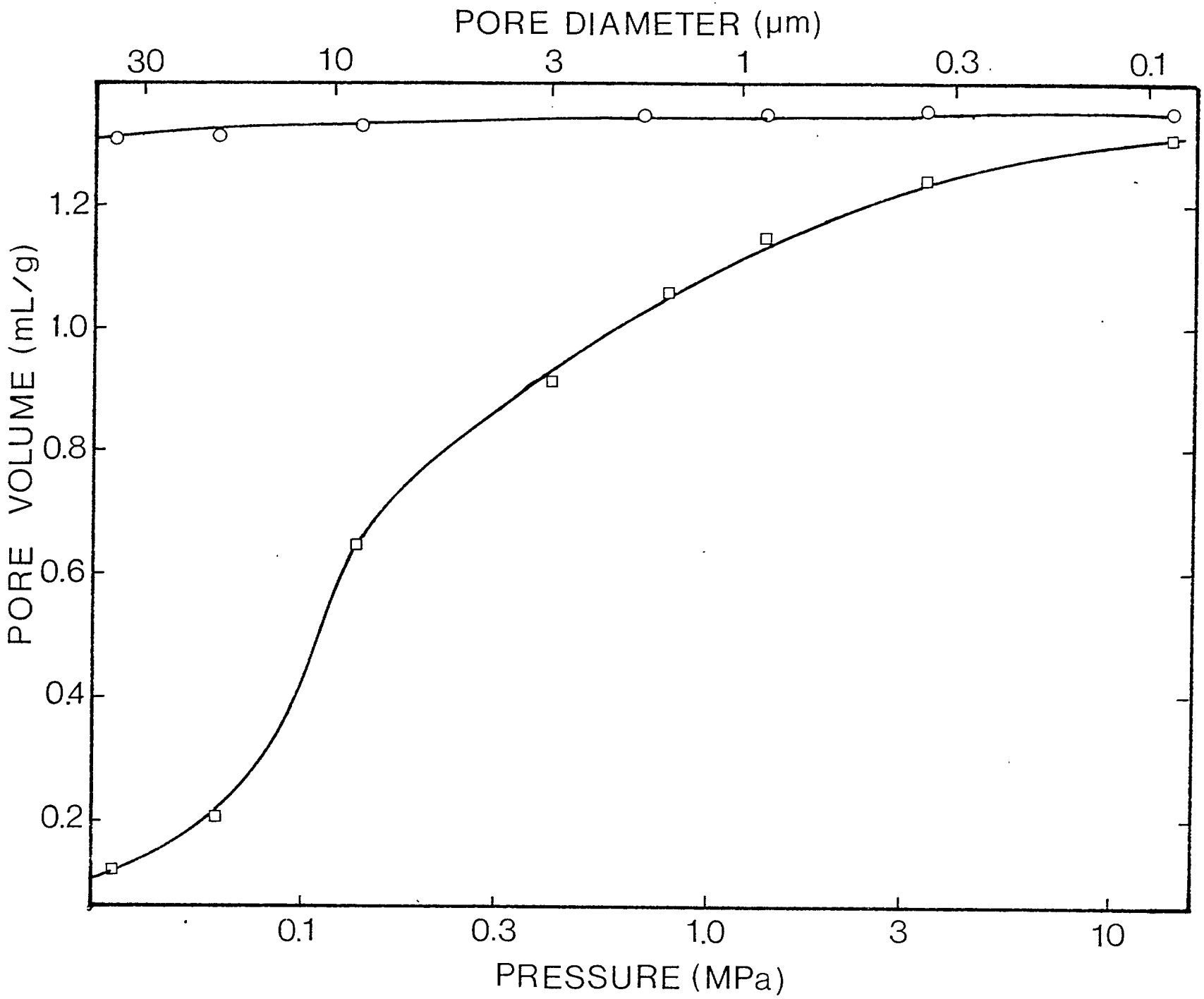
PORE DIAMETER (μm)
30
10
3
1
0.3
0.1
PORE VOLUME (mL/g)
1.2
1.0
0.8
0.6
0.4
0.2
0.1
0.3
1.0
3
10
PRESSURE (MPa)

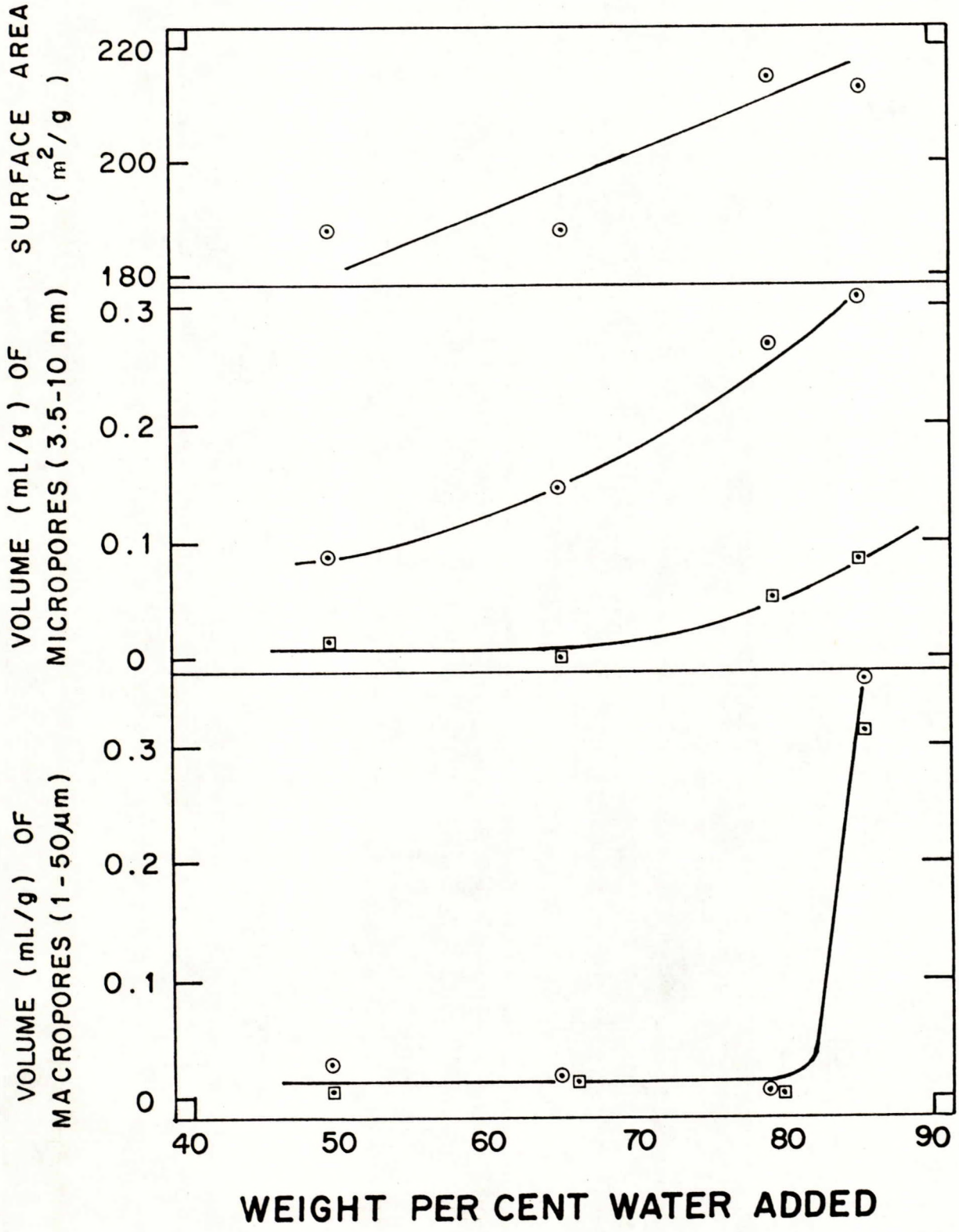
SURFACE AREA (m^2/g)
220
200
180
VOLUME (mL/g) OF MICROPORES (3.5-10 nm)
0.3
0.2
0.1
0
VOLUME (mL/g) OF MACROPORES (1-50μm)
0.3
0.2
0.1
0
40
50
60
70
80
90
WEIGHT PER CENT WATER ADDED

FIGURE 3

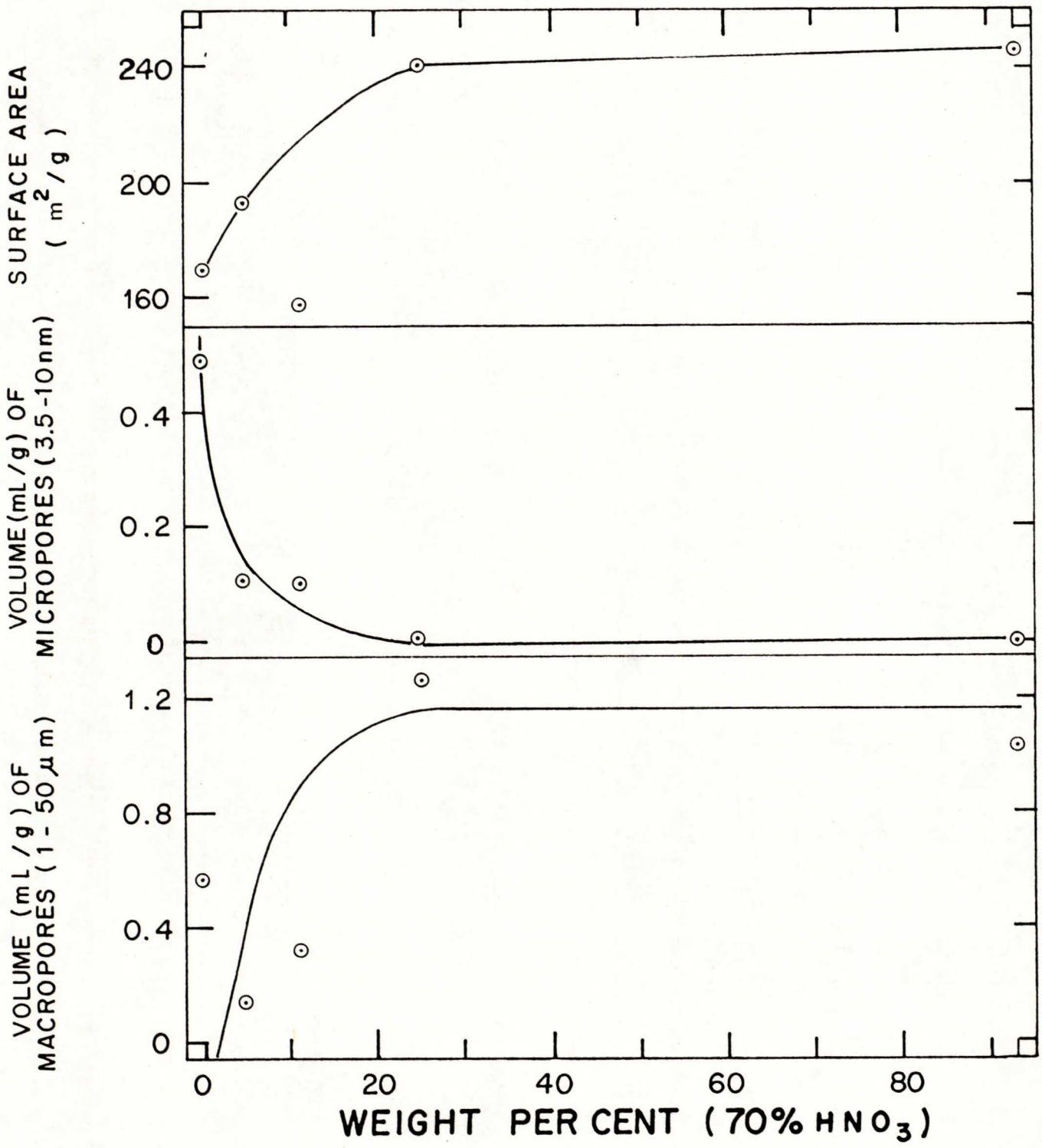
SURFACE AREA (m^2/g)
240
200
160
VOLUME (mL/g) OF MICROPORES (3.5-10nm)
0.4
0.2
0
VOLUME (mL/g) OF MACROPORES (1 - 50 μm)
1.2
0.8
0.4
0
0
20
40
60
80
WEIGHT PER CENT (70% HNO_3)

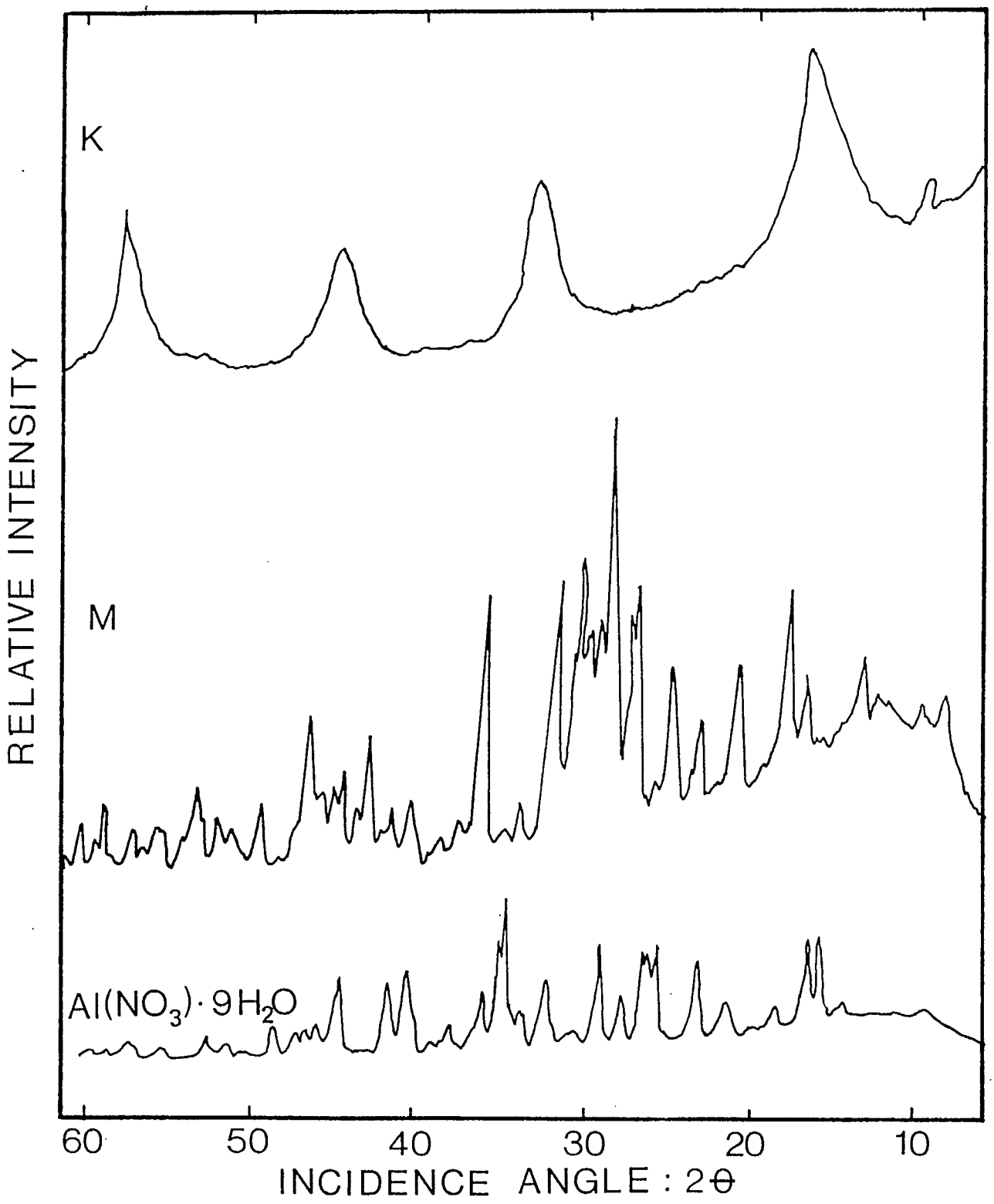
K
M
Al(NO3)·9H2O
RELATIVE INTENSITY
60
50
40
30
20
10
INCIDENCE ANGLE : 2θ

FIG 3

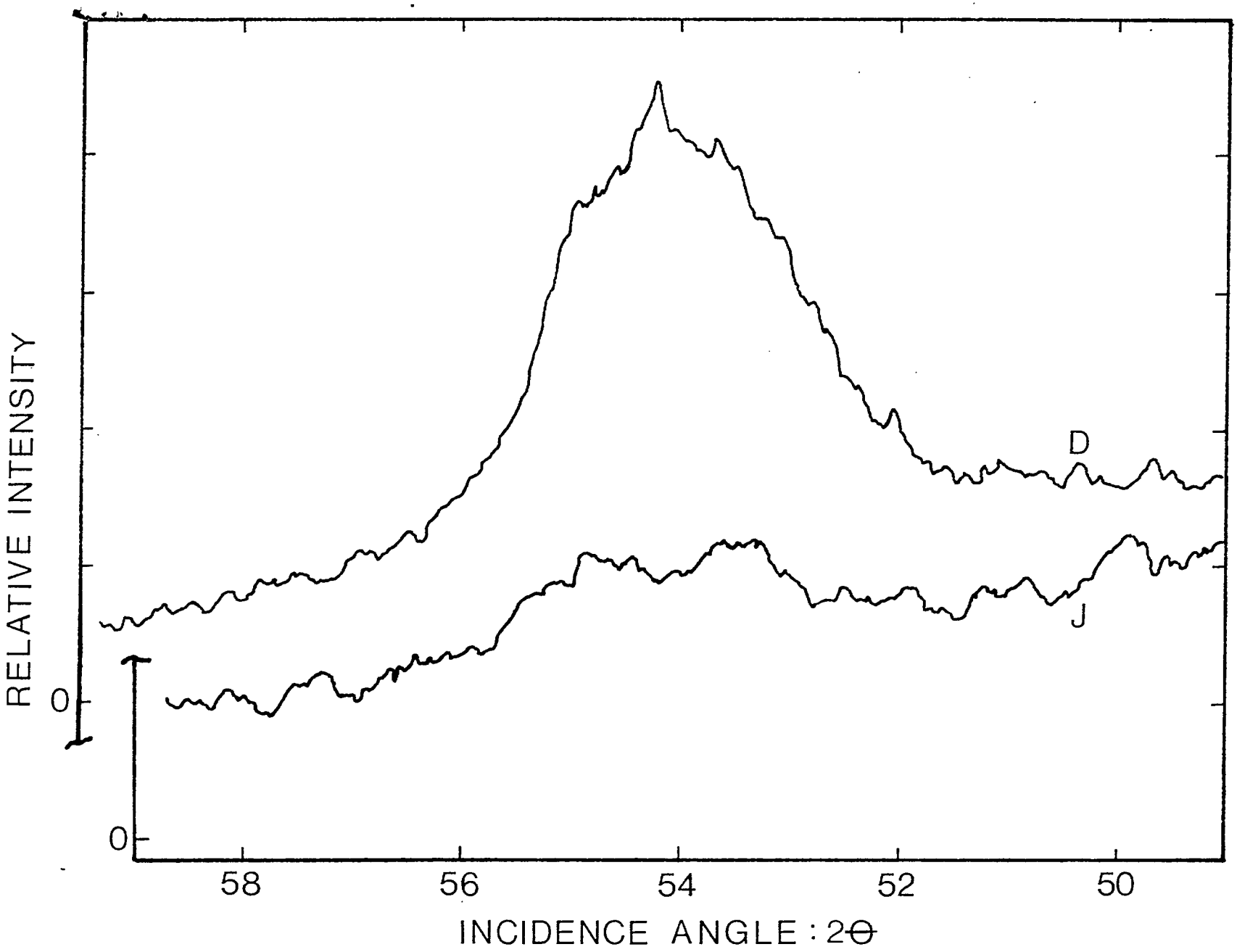
RELATIVE INTENSITY
D
J
0
0
58
56
54
52
50
INCIDENCE ANGLE : 2θ

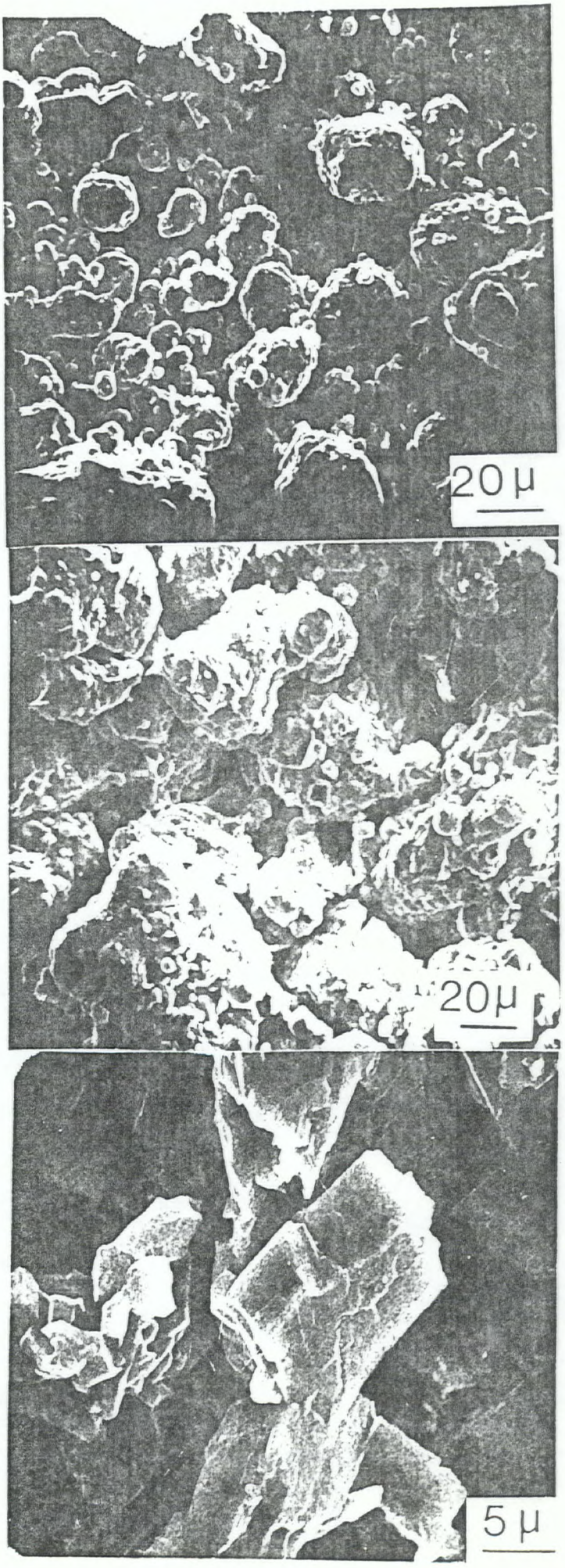
20 µ
20µ
5 µ

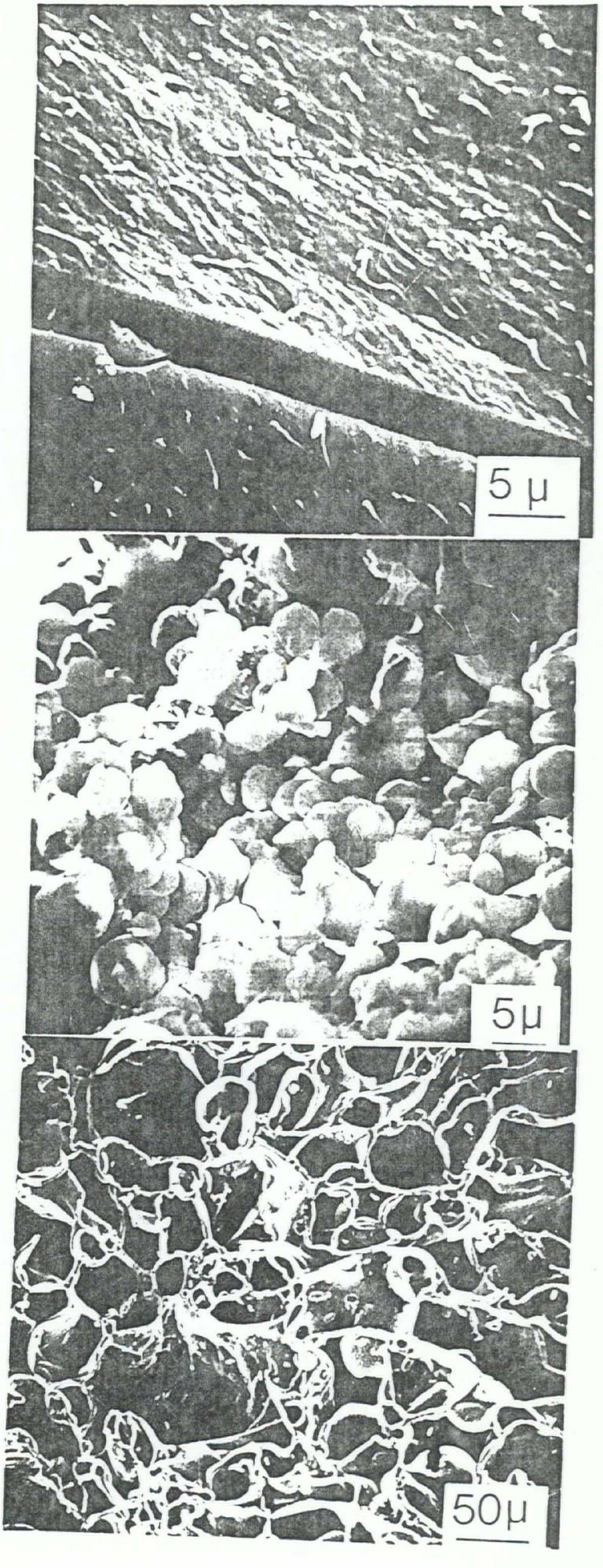
5 µ
5µ
50µ

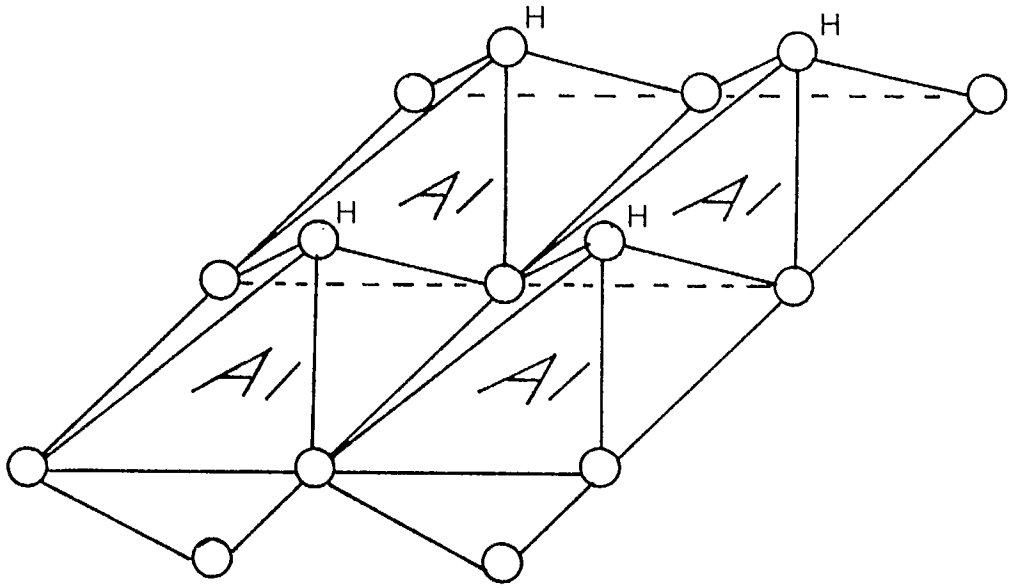
H
H
H
H
Al
Al
Al
Al

(a)

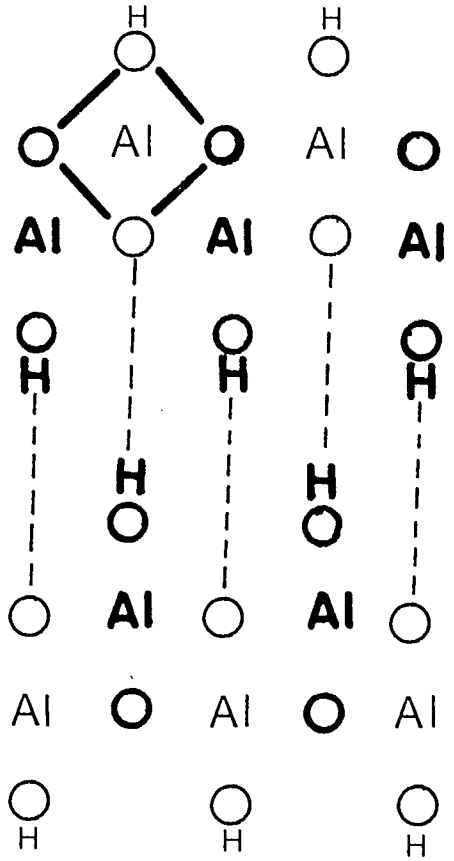
H
H
Al
Al
O
O
Al
Al
Al
OH
OH
OH
H
O
H
O
Al
Al
Al
Al
O
O
Al
H
H
H

(b)

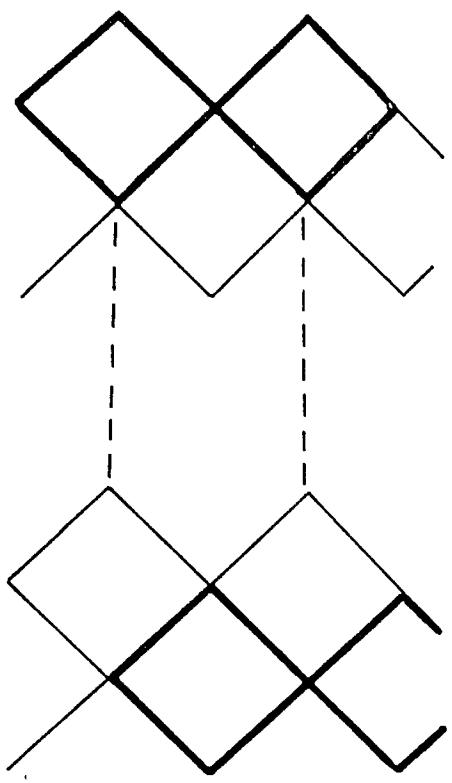

(c)

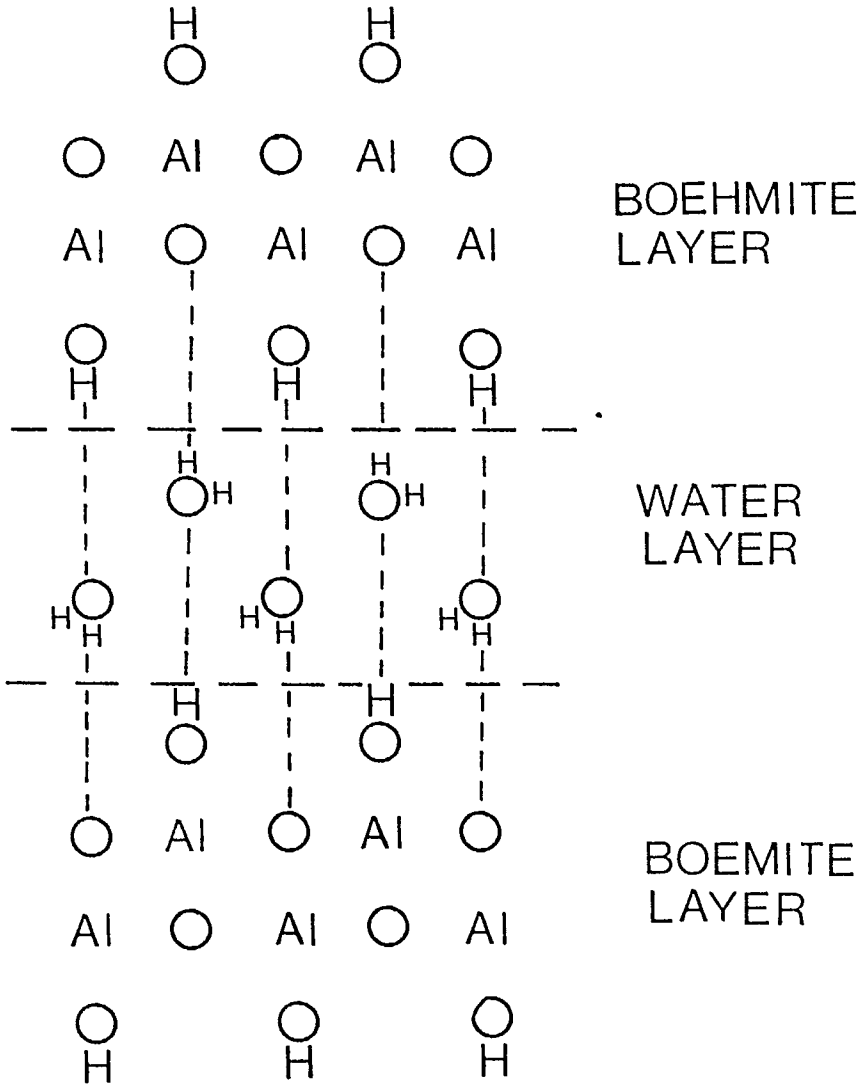
BOEHMITE LAYER
WATER LAYER
BOEMITE LAYER